Effects of Boundary Conditions and Posture on Simulations with Human Body Models of Braking Events

N. Erlinger, D. Kofler, E. Heider, C. Klug

Abstract The aim of this study was to investigate the effects of boundary conditions and postures in simulations with human body models (HBMs) when replicating volunteer tests in an occupant environment. Data from sled tests with a peak acceleration of about 0.5 g from male volunteers seated in a backward mounted seat in passenger posture were used for this study. A stepwise approach was taken for the positioning of the HBM by gradually adjusting the original HBM in driver posture to the subject's posture as target, since this made it possible to specifically study the influence of the posture of certain body regions. The simulations were run with different HBM versions (THUMS V4, THUMS V5, THUMS V6) in passive state (no muscle activation) and with V5 and V6 in active state (relaxed/reactive). The responses from different HBMs were generally consistent. The leg posture showed a comparatively smaller influence than the arm posture. In general, it was observed that more movement between the wrists and the thighs resulted in larger head excursions, suggesting torso support via this loading-path. In addition, the seat model was identified to play a major role on peak head excursion when compared to simplified modelling approaches.

Keywords autonomous braking, Human Body Model, HBM, passenger, volunteer test.

I. INTRODUCTION

More than half of all accidents with passenger cars are associated with evasive manoeuvres, whereas the most common reaction is braking [1–3]. Furthermore, autonomous braking assistant (AEB) systems are mandatory within the European Union for new car models by the year 2022 and for all new registrations by the year 2024 [4]. Deceleration of the occupant due to braking is affecting the initial posture prior to the accident and is therefore relevant for the design and assessment of restraint systems [5]. Considerable differences in forward excursion between volunteers and a Hybrid 3 (H III) 50th percentile male dummy were shown [6–7]. Conventional crash test dummies have no muscle activity and are stiffer at lower severities than human body models (HBMs) [8]. Passive HBMs (without muscle activity) were extensively validated using experimental data by post mortem human subjects (PMHS) with a focus on in-crash applications [9]. The pre-crash forward head excursions of passive HBMs were shown to be comparable to PMHS results rather than to volunteer responses [9–11] as muscle activation plays an important role for acceleration levels typically resulting from braking manoeuvres [7].

The ability of active HBMs to represent volunteer behaviour had been shown in multiple studies using mostly in-house developed models [12–15]. The active Total Human Model for Safety (THUMS) V5 was released in 2015 as the first widely available active HBM to expand the field of application of THUMS to acceleration levels e.g. occurring at braking manoeuvres [12]. It includes 262 Hill-type muscles as 1D elements. The muscle modelling was later revised based on a proportional-integral-derivative (PID) control loop mechanism, as implemented in LS-DYNA [10]. Volunteer tests by [16] were used for fitting the PID gains parameters [17–18]. The implementation of two separated controllers (posture control and reaction force control) led to a good reproduction of both relaxed (posture control) and braced (reaction force control) volunteer responses [10–11, 19]. The muscle model of THUMS V5 was eventually adapted to the more detailed passive THUMS V4 and released as THUMS V6 [11]. THUMS V4 (passive) and V6 (passive and active) feature the anthropometry of an individual close to a 50th percentile male. Computer-tomography (CT) scans from a 39 year old volunteer (77.3 kg, 173 cm) were used for the modelling of the human body [20]. THUMS V5 is based on a different anthropometry and represents a more generic 50th percentile male model, since the geometry was scaled to a 50th percentile male adult based on the anthropometrical measurements by [21] (74 kg and 175 cm) [12].

Corina Klug is Assistant Professor (email: corina.klug@tugraz.at, phone: +43 316 873 30329), Nico Erlinger, Desiree Kofler and Eva Heider are Research Assistants at the Vehicle Safety Institute at Graz University of Technology, Austria.

For the calibration and validation of such active HBMs, volunteer test data is needed. Volunteer tests of braking events are conducted in both driving passenger cars and on seats mounted on sled systems in a laboratory environment. Tests in passenger cars have the advantage that they are performed in the most realistic environment, with the volunteer situated in a high and potentially completely unaware state, i.e., study masked as ergonomic research. However, they may have some shortcomings when it comes to measuring possibilities, i.e., trajectories of multiple body parts such as head, arms and legs.

Investigation of volunteer response to braking events in passenger cars have generally been done in connection with initial relaxed muscle conditions at full braking events (approx. 1.0 to 1.1 g) [6, 22–29], at multiple deceleration levels (3, 4, 5 m/s²) [30] or the volunteers applying the brake pedal by themselves [31]. With seats mounted on sled systems, differences in the response of relaxed and braced muscle states of volunteers have been investigated at various acceleration levels: 0.2 g, 0.6 g and 1.0 g [32]; 0.8 g [3, 33]; 0.82 g [34]; 1.0 g and 2.5 g [35] and 2.5 g and 5.0 g [7, 16]. Screened volunteer studies featuring pre-crash related acceleration pulses had different levels of experimental details and documentation included in the publications. While some studies reported detailed initial postures and trajectories for each volunteer, some authors included only exemplary data or averaged data. For both detailed instrumented sled tests and tests in passenger cars, full datasets are often not published, which would be necessary to reproduce them virtually for calibrating or validating active HBMs.

It is unclear how unknown boundary conditions and the posture affect the HBM results and therefore the overall validation result when using volunteer tests. The objective of this study was to identify the key influencing parameters of the simulation setup that affect the kinematics of different HBMs as a means of developing guidelines for future tests and validation simulations. From this objective, the following specific research questions were defined for the presented simulation study:

- Which posture targets and simulation boundary conditions are most relevant for simulations with active and passive HBMs when replicating low-severity volunteer tests?
- Are potentially existing differences of the HBM responses caused by variations of boundary conditions and posture consistent among different HBMs?

The effect of the simulation setup was investigated using a well-defined, publicly available volunteer test dataset [36]. A secondary aim of this paper was to provide guidelines on how this dataset could be used by other researchers in the future for validation or calibration of active HBMs.

II. METHODS

On basis of the research questions, various parameters were identified for further investigation and included in the parameter study. Variations of the parameter were run with different postures and with different HBMs, including both active and passive muscle states. The utilisation of open tools available free of charge was focused on and carefully researched for the simulation study. The test data from volunteer tests selected for the simulation study included a comprehensive documentation and measurement data, e.g., trajectories, electromyography (EMG), force signals [36]. Also, an extensively calibrated version of the utilised seat model had been made publicly available by the authors on the OpenVT platform (https://openvt.eu) [37]. In addition, the utilised positioning tool is also publicly available on the OpenVT platform [38]. Post-processing was done with the opensource tool Dynasaur [39]. Finally, utilised HBMs (THUMS) are available upon registration without charges [40].

A. Experimental Volunteer Sled Tests

A detailed dataset of sled tests representing brake events with six male volunteers (see Table I for descriptive data) conducted in a laboratory environment was chosen to serve as a basis for the HBM simulations. Approval of the local ethics committee of the Medical University of Graz, Austria, (EK 30-157 ex 17/18) for the volunteer tests have been granted. A padded generic seat facing backwards was mounted on a sled system and was accelerated to a peak velocity of 3.3 m/s. The ramp-up time of the pulse was 0.33 s, with the maximum acceleration of 0.47 g with a steady-state time of 0.72 s (see Appendix A, Fig. A-1). The overall test duration limit was the same for each volunteer. Due to continuous adjustments to the time schedule, the number of experiments for each volunteer varied between two and four, resulting in a total of 19 experiments. The volunteers were instructed to relax and were unaware of the exact acceleration onset. Targets for visual tracking were attached at major anatomical landmarks (shown in Fig. 1, full names of landmarks listed in Appendix A, Table A-I). The following landmarks are subsequently referred to as wrist for WRSL, knee for KSL and head for HA. The tests were recorded with a stereo high-speed camera setup. Furthermore, the pressure on the seat was

measured during the test with pressure measurement mats (LX100:40.40.02, XSENSOR, Calgary, Canada) on seat and back surfaces. Muscle activity of the volunteers was captured by non-invasive surface electromyography (EMG) (see Appendix A, Fig. A-2 for overview of muscles).

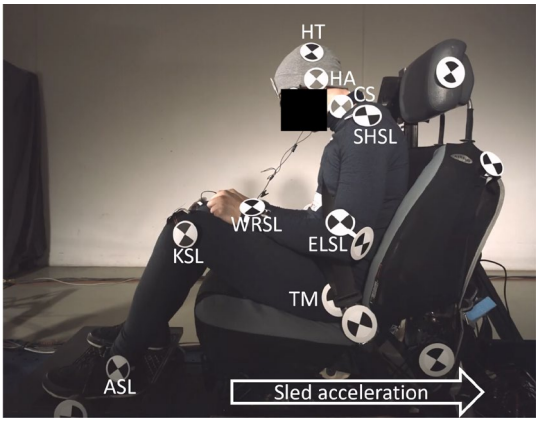

Fig. 1. Photo of a volunteer (P03) on the test seat mounted on a sled at the time of peak forward head excursion in Test 03.

TABLE I
DESCRIPTIVE DATA OF THE MALE VOLUNTEERS

Volunteer	*Weight [kg]*	*Age [yr]*	*Height [cm]*
P01	74.2	33	172
P02	73.3	29	171
P03	73.3	30	175
P04	76.8	33	172
P05	73.4	25	178
P06	80.1	33	173
Mean	75.4	30.5	174

B. Finite Element Simulation Models

The tests of volunteer P03 (73 kg, 175 cm) were selected as candidate for the HBM simulations, as excursions were found to be comparable to other test in the literature [32, 34] and the volunteer was not pre-tensed according to the EMG data analysis. These tests will be subsequently referred to as Test 01, Test 02 and Test 03 (originally labelled P03T01, P03T02 and P03T03). Acceleration-time history of Test 03 was prescribed in all simulations (see Appendix A, Fig. A-1 for acceleration over time plot).

1) Occupant HBMs

Different HBMs were used for simulations, representing slightly different anthropometries, active and passive models: THUMS Version 4.02 (subsequently referred to as THUMS V4), THUMS Version 5.03 (THUMS V5) and THUMS Version 6.02 (THUMS V6). Whereas THUMS V5 and THUMS V6 were used without muscle activation (referred to as passive) and with reactive muscles (named initially *relaxed* by the model developers [11]).

Posture adjustments of the HBM were carried out in dedicated positioning simulations. A publicly available simulation-based positioning method by [41] was used for reproducible positioning of the HBMs. This method allows direct input of the landmark coordinates for the target posture, as it takes the anthropometrical differences between HBM and volunteer into account and calculates the adjustments needed. Landmark coordinates of the volunteer target posture are shown in Appendix A (Table A-I). For positioning simulations, a prescribed motion was applied via beam elements to nodes of the cortical bones of the HBM. The positioning simulations were run for a simulation time of 0.4 s with ramped displacement. Nodal coordinates of the last time step were exported for each posture of THUMS V5 and THUMS V6. No positioning simulations were run with THUMS V4 as nodal consistency allowed the import of THUMS V6 nodal coordinates. The nodal coordinates of the positioned models were integrated into the original models without further smoothing.

The muscle complex of the active HBMs requires additional efforts when positioning via pre-simulations [42]. Muscle-related positioning procedures were carried out as suggested in the official THUMS documentation [17–18]. Initial joint angles were read from the *curvout* data of the positioned HBMs and used for updating the parameters in the respective simulation input files. Moreover, the IDs of swapped seatbelts were updated. The seatbelt elements did not potentially meet the requirements for the initial length for initialisation after the positioning procedure. The affected elements were elongated by means of translating nodes along the seatbelt direction. Finally, the nodes of rigid bodies used for the definition of spherical joints in the upper extremities were set in a precisely coincident manner to avoid possible errors resulting from slight differences in nodal coordinates (applies only to THUMS V5).

2) Sled and seat models

For the development of the seat model, the geometry was digitised by a laser scanner (Quantum Max, FARO, FL, US). Material tests of the foam material were conducted and used for calibration of the material parameters.

Translational springs in all coordinate directions represent the stiffness of the mounting structures between the seat and the sled. Although a standard three-point seat belt was used in the experimental test, the belt was not included in the available seat model. Locking of the retractor was not observed in the volunteer tests, and no notable belt forces were measured in the experiments. The influence on the HBMs was thus assumed to be negligible.

C. Simulation with HBMs and Postprocessing

The first 0.2 s of the simulations were used for settling the HBM on the seat. The positioned male 50th percentile HBMs was placed close above the seat (contact thickness plus one additional millimetre) and different settling procedures were applied, which are described in section D. Thereafter, the velocity of all the nodes was reset to zero, to minimise seating procedure-related movements. The position of the footrest for each HBM posture and HBM version was adjusted to provide comparable foot support. A simulation of the settling phase without the footrest was run in order to identify the exact location of the footrest for the settled HBM. The acceleration curve obtained from experimental data (Test 03, see Appendix A, Fig A-1) was prescribed. Therefore, the acceleration-time history was applied to the rigid plate under the seat in the longitudinal direction, while motion in other directions was constrained.

The publicly available post-processing tool Dynasaur [39] was used for evaluation of the HBM response. Node histories of anatomical landmarks were defined. In contrast to the volunteer tests, the nodes of cortical bones were selected to enable a more comparable analysis among different models and neglect the effects of potentially occurring soft tissue deformations from different postures. The used nodes are shown in Appendix C (Fig. C-1 and Table C-1). All simulations were run with LS-DYNA MPP R9.2.0 (LSTC, Livermore, CA, USA) with single-precision on a Linux HPC cluster.

D. Simulations with Varying Posture and Boundary Conditions

The different responses of the HBMs were first examined individually and then combined to finally investigate the mutual effects of both posture and boundary conditions. A baseline simulation was defined for the simulations where only one parameter was varied, using the following parameters: deformable seat (def), gravity-based settling, skin friction coefficient of 0.3, seat friction coefficient of 0.5. Furthermore, the arms-legs-back (ALB) posture was used as the baseline.

1) HBM posture

Positioning of the HBMs was done based on a stepwise approach. In addition to the default driver posture (D) and the volunteer-specific posture (ALB), three intermediate postures were included: positioned arms (A), positioned legs (L) and positioned arms and legs (AL) as shown in Fig. 2. Therefore, only the respective body parts were moved in respective positioning simulations, while the movement of nodes belonging to the cortical bones in unaffected body parts was constrained.

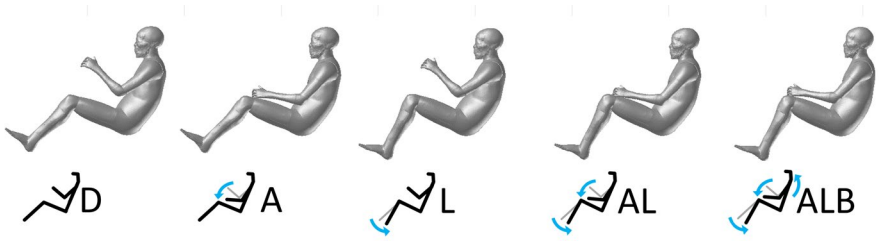

Fig. 2. Stepwise positioning of the HBM to the target posture from volunteer ALB including three intermediate postures (abbreviations: D (driver), A (arms), L (legs), AL (arms and legs), ALB (arms, legs and back)).

The ankle posture was not adjusted during the positioning process, because initial simulations revealed stability issues if this was done. The angle between the foot and the lower leg therefore remained constant for all postures. The posture described by angles between the landmarks (absolute values relative to horizontal) for the volunteer postures and of the applied HBM postures are shown in Table II. For comparability to volunteer posture, measurements of the HBM posture were conducted after gravity-based settling on the seat rather than directly after positioning. Settling caused changes to the angles, with these mainly related to the torso and head up to 3 deg. Notable differences resulted for angle between CS-SHSL, which were caused by deviation of the C5 landmark position relative to the vertebra between test and HBM. The spinous process of the 5th cervical vertebra was used for identification of the landmarks by the volunteers, however, due to the size of the target it was placed

in a more anterior location. The definition for the HBMs remained at the spinous process (see Appendix C (Table C-I) for node IDs), as the target coordinates of CS were not included in positioning.

TABLE II
DESCRIPTION OF HBM POSTURES AFTER SETTLING AND VOLUNTEER POSTURE BY ANGLES BETWEEN LANDMARKS.
*ALB POSTURE, ** NOT CONSIDERED BY POSITIONING

Angle [deg]	*Volunteer P03 T02/T03*	*THUMS V4/V6*		*THUMS V5*	
		Driver	Positioned	driver	Positioned
*HA-CS **	88/88	86	86	89	89
*CS-SHSL **	81/87	69	66	75	73
SHSL-ELSL	60/59	41	56	44	59
ELSL-WRSL	4/3	40	5	38	7
CS-TM	69/70	66	66/71*	66	66/69*
TM-KSL	23/23	22	26	22	25
KSL-ASL	63/62	42	60	45	61

2) Seat modelling

Modelling a production seat generally includes the digitisation of the geometry involved, e.g. with laser scanner and material testing together with subsequent calibration of the material parameters. A production seat may thus be a time-consuming task in terms of the documentation and the modelling work required. Moreover, a rigid seats comprised of two flat surfaces had been used for previous volunteer tests on acceleration sled systems [2, 32, 35] or in a passenger car [25]. Three seat models were included in the simulation study starting by the simplest modelling these seats are:

- Rigid flat (flat rig): the seat model consists of two plates (shell elements, rigid steel material properties) matching the angle between the seat and back surfaces of the test seat (103 deg.).
- Rigid geometry (geo rig): the seat model used the full geometry of the seat, but the outer shell layer (originally leather covering) was switched to the rigid material of the rigid flat seat and solid foam elements of the seat model were removed.
- Full deformable (def): the seat is the virtual representation of the seat used for tests with respect to both geometry and material.

In addition, pressure between the HBM and the seat was compared to experimental data by volunteer P03. A slight asymmetrical seat geometry (revealed by analysis of the laser scanned geometry, but not by visual inspection of the actual seat) of the seat surface was used, rather than the symmetric geometry (mirrored) of the seats included in the simulation study. Solid element stress perpendicular to the seat facing after gravity-based settling of the HBMs (THUMS V4 and V5, both in posture ALB) was used for plotting the pressure distribution.

3) Friction coefficient of arms to thigh contact

As differences in arm motion were observed between the tests, the effect of such movements and the force between arms and legs was analysed by varying the coefficient of friction of the contact definition. Simulations were run with values 0.1, 0.3, 0.5 and 1.0 of the friction coefficient *FS* (with the decay coefficient *DC* set to zero, so independent of relative velocity).

4) Settling method

Within the settling process it is aimed to reach realistic reaction forces close to a static equilibrium (gravity force equals reaction force of the seat) before onset of the prescribed acceleration. Gravity based approaches [9, 12, 43] but also prescribed motion-based methods had been applied [41]. Therefore, the baseline method of gravity-based settling (ramping up gravity within 0.2 s) was compared with settling by prescribed motion. The script *Positioning_FE_2_model_CNRB.py* of PIPER Version 1.0.2 [44] was used for creating a high number of beams, e.g. 4538 beams for THUMS V4, that were attached to nodes distributed to all the cortical bones. This method had originally been intended for posture adjustment by dragging the body parts three-dimensionally into a desired position. In this study, prescribed motion was only applied in the z-direction for settling. Data of the volunteer tests (load cells below seat and footrest) showed that the volunteer had 83% of his body weight resting

on the seat while seated stationary, with the remaining 17% resting on the footrest. Corresponding values for the HBMs were close to 80% of the respective body weight on the seat, and therefore used for the calculation of required displacement by prescribed motion (606 N for THUMS V4/V6 and 581 N for THUMS V5). Starting by the initial position of the HBM above the seat, prescribed motion with a magnitude of 44 mm (THUMS V4/V6) and 35 mm (THUMS V5) was applied in the z-direction within 0.2 s, in order to reach the respective target force.

5) Friction coefficient of the seat contact

No trajectory via automated target tracking of the stereo video data from the tests was available for the landmark Trochanter Major, since the target was occluded by the belt buckle. This may be a challenge of a general nature in volunteer tests of similar type. Furthermore, the friction coefficient between volunteer and seat depends on the clothes worn by the volunteers and is difficult to determine especially when using pressure mats. The parameter variation was conducted in order to analyse the pelvis movement relative to the seat when modifying the friction coefficient of the corresponding surface-to-surface contact. The static friction coefficient *FS* was set to values of 0.3, 0.4 and 0.5, respectively.

III. RESULTS

A. Volunteer Responses of Experimental Sled Tests

The peak forward head excursions of the volunteers caused by the acceleration pulse showed to be very subject-specific and were in the range from 34 to 514 mm. Fig. 3 shows the peak values for each volunteer as a black dot, in addition the subject specific range is highlighted with a grey bar (blue for P03). The following mean peak excursion of the head were measured for the volunteers: 35 mm (P05), 50 mm (P02), 60 mm (P01), 119 mm (P06), 230 mm (P03) and 462 mm (P04). However, variations between repeated tests of the same volunteer were comparably small (mean range of the volunteers 61 mm, SD 36 mm). Forward head excursions over time are plotted in Appendix B (Fig. B-3).

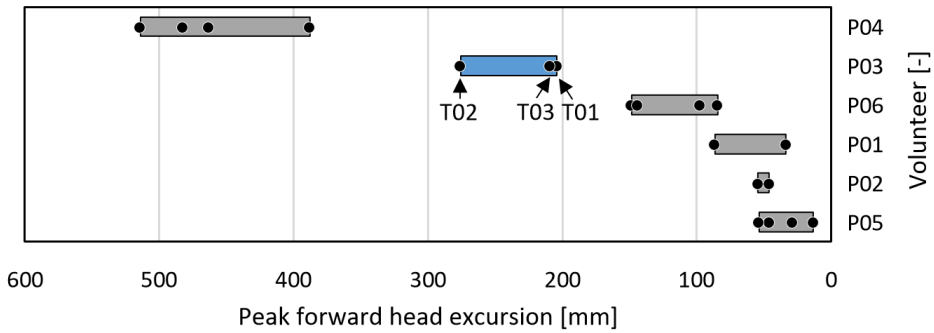

Fig. 3. Peak forward head excursions of the repeated tests of the volunteers. Horizontal grey bars show the range of excursion for each volunteer. The range of the selected volunteer (P03) is highlighted in blue with labelled test numbers (T01, T02, T03).

B. Baseline Simulations Compared to Volunteer Results

Peak forward excursion of the landmarks head, wrist and knee of the HBMs (posture ALB, aimed at matching all angles of the volunteer tests) are compared with two tests of volunteer P03 in Fig. 4. The simulations showed general excursions close to those observed in the volunteer tests (head: 196 mm, 276 mm), especially for the reactive HBMs. For the head peak excursions of the reactive HBMs of 143 mm (THUMS V5) and 278 mm (THUMS V6) were measured, whereas for passive HBMs the excursion was 408 mm (THUMS V4), 450 mm (THUMS V6) and 495 mm (THUMS V5). As the peak acceleration level of 0.47 g indicated, excursions were highly driven by muscle activity causing the differences between passive and reactive THUMS V5 and THUMS V6.

Peak forwards excursion of the wrist of volunteer P03 were 17 mm without sliding on the thighs (Test 03) and with sliding 140 mm (Test 02). Sliding motion of the hands was observed in all simulations in posture ALB in the baseline configuration in different extents, resulting in a range of 52 mm (reactive THUMS V5) to 156 mm (passive THUMS V5). See Section D for more details on the relative motion between the hands and the thigs of the HBMs. For volunteer P03 a peak excursion of the knee of 8 mm (Test 03) and 17 mm (Test 02) was measured. For this landmark the range of the HBMs was 10 mm (reactive THUMS V5) to 24 mm (passive THUMS V5). A visual

comparison of the volunteer and the HBM responses is shown in Appendix B (Fig. B-1) together with both two-dimensional head trajectories (Fig. B-2) and forward head excursions over time (Fig. B-3).

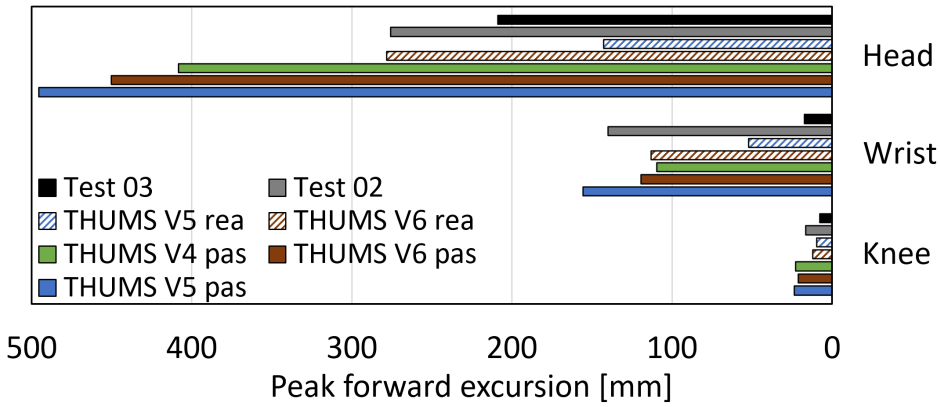

Fig. 4. Peak forward excursion of Tests 02 and Test 03 compared to HBMs (right) for the landmarks head, wrist and knee (Abbreviations: pas … passive, rea … reactive).

C. *Influence of HBM Postures*

Peak forward head excursion was evaluated for the five postures of all HBMs in order to investigate the impact of the stepwise positing approach. The trends observed in the course of this were in general comparable for the different HBMs. The driver posture (D) of the respective model was set as a baseline for the calculation of relative changes to the peak forward excursion as shown in Fig. 5. Values of the peak forward excursion are shown in Appendix B (Table B-I). All four postures caused a decrease of peak head excursion compared to posture D. Positioning of only the arms on the thighs (posture A) caused a reduction of 23% and 24% for THUMS V4 passive and THUMS V6 passive. For THUMS V5 peak head excursion was reduced by 46%. The reactive HBMs (THUMS V5 and V6) were affected by a reduction of 61% and 59% respectively. For the posture L, the decrease of peak head excursion was comparable for all HBMs ranging from 9% to 13%. The three passive HBMs had comparable results for posture AL resulting in a decrease of peak head excursion by 26% to 28%. Reactive THUMS V5 and reactive THUMS V6 showed a decrease of 65% and 80%, respectively. However, in posture ALB these clear differences between passive and reactive HBMs vanished and all models showed relative reduction in the peak forward excursion in a range of 24% to 33%.

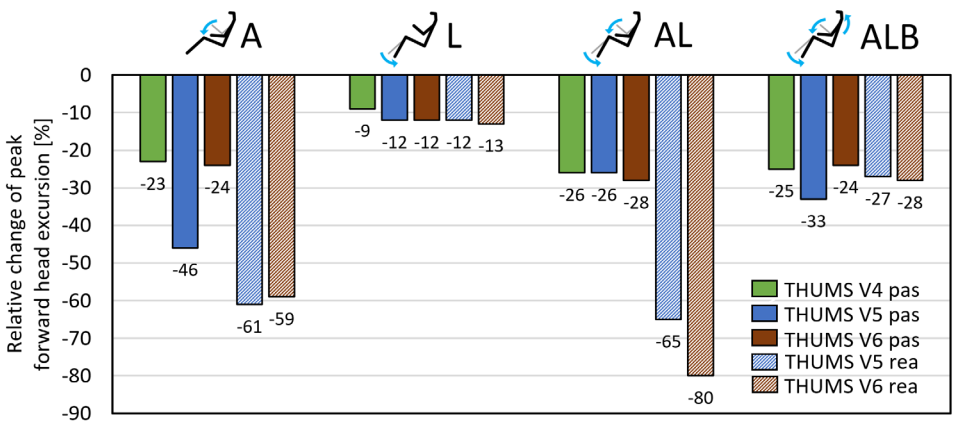

Fig. 5. Relative change of peak forward head excursion of the original driver posture (D) to the postures A, L, AL and ALB

D. *Effect of Varying Boundary Conditions*

1) *Friction coefficient of arms to thigh contact*

Variation of the friction coefficient between arms and thighs caused major differences in the wrist peak excursion and the head peak excursion, also depending on the influence of the posture. For the friction coefficient of 0.1, the relative movement between hands and thighs is clearly visible during a visual inspection, whereas the

increased friction coefficients led to lower relative motion. Both, passive THUMS V4 and reactive THUMS V5 showed a reduction of head excursion and decreased wrist excursion due to increased skin friction coefficient. Wrist excursion below approx. 60 mm (THUMS V4) and approx. 20 mm (THUMS V5) is almost exclusively caused by elastic soft tissue deformation of the thighs rather than by sliding. Fig. 6 shows cross-plots of the head peak excursion and the wrist peak excursion for passive THUMS V4 (left) and reactive THUMS V5 (right).
When comparing the peak excursions for the friction coefficients 0.1 and 1.0, the following results were observed for posture ALB: Passive THUMS V4 showed a lower head excursion of 430 mm compared to 393 mm (-9%) in connection with a reduction of wrist excursion by 95 mm (-70%). The reactive THUMS V5 showed a change of head excursion from 178 to 118 mm (-34%) while wrist excursion was reduced by 58 mm (-73%).

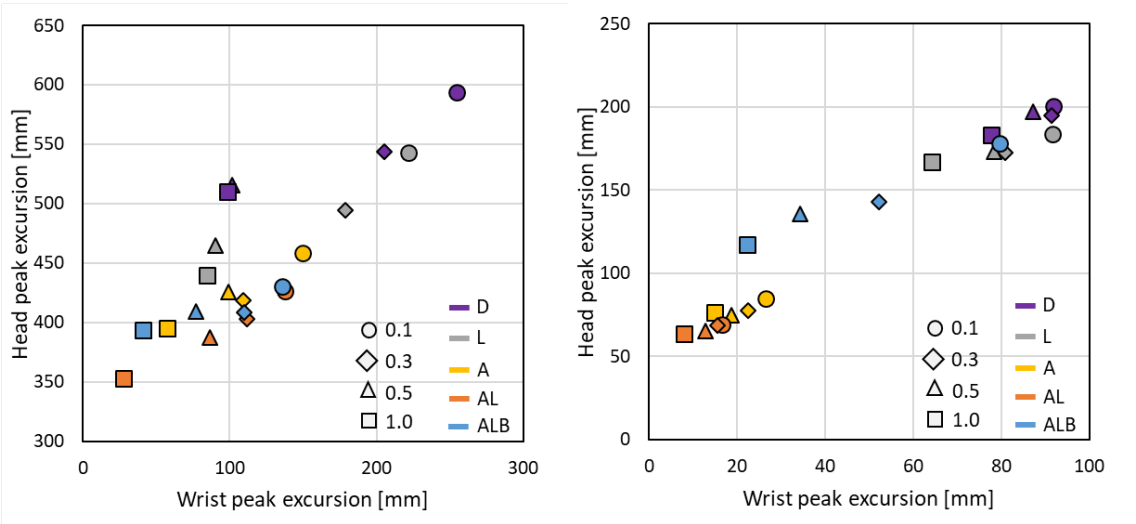

Fig. 6. Cross-plots of peak excursions of landmarks on head and wrist for friction coefficients (0.1, 0.3, 0.5, 1.0) and postures (D, L, A, AL, ALB) for passive THUMS V4 (left) and reactive THUMS V5 (right).

2) Seat modelling

The effect of the seat type is shown as a cross-plot of peak head excursion over peak Trochanter Major excursion. The reactive THUMS V5 (Fig. 7, left) showed a higher sensitivity to the type of seat (deformable (def), geometric rigid (geo rig) and flat rigid (flat rig)) compared to the passive THUMS V4 (Fig. 7, right). Peak excursion of both the Trochanter Major and the head increased due to simplification of the deformable seat (def). For posture ALB, peak head excursion of passive THUMS V4 increased from 408 mm (def) to 492 mm (flat rig) and 516 mm (geo rig). For reactive THUMS V5 the seat model caused larger relative changes than for passive THUMS V4. Peak head excursion of ALB posture was 143 mm (def), 225 mm (flat rig) and 263 mm (geo rig).

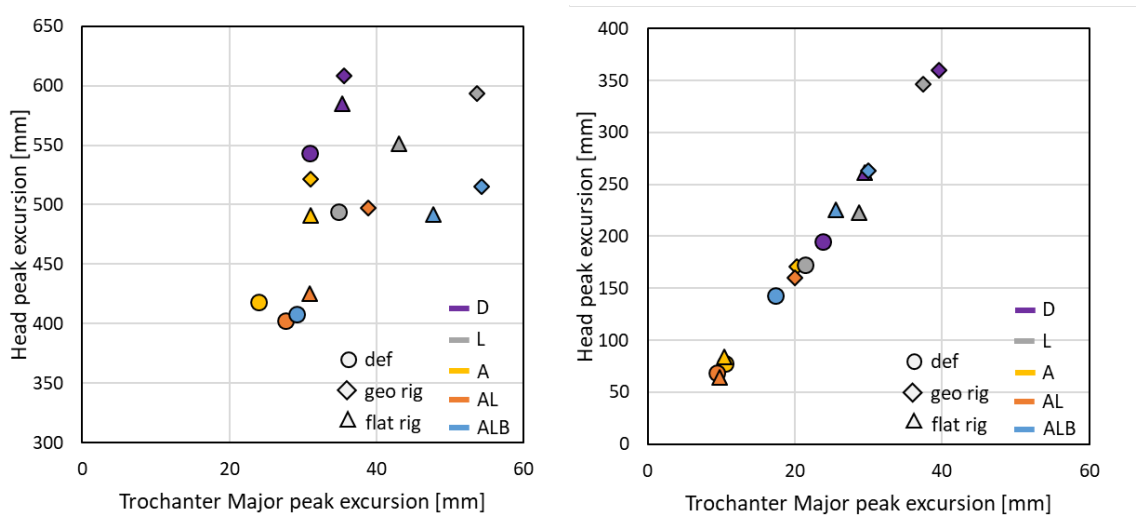

Fig. 7. Cross-plots of peak excursions of landmarks on head and Trochanter Major for three seat types (def, geo rig, flat rig) and postures (D, L, A, AL, ALB) for passive THUMS V4 (left) and reactive THUMS V5 (right).

3) Settling method

Cross-plots of peak excursion of the head comparing both settling methods are shown in Appendix E (Fig. E-1). In addition, contact force over time for both settling methods is plotted in Appendix E (Fig. E-2). Prescribed motion settling caused an additional movement of the HBM after the settling phase (for approx. first 0.05 s). Slight movement of the HBM also occurred, however, during gravity-based settling. Both HBMs adapted to the influence of gravity that resulted in a slight hunchback. Differences of the peak head excursion compared to gravity-based settling were observed for posture ALB. In numbers the comparison of gravity-based settling with the prescribed motion gives: +12 mm (+3%) for passive THUMS V4 passive and -6 mm (-4%) for reactive THUMS V5 relaxed. This tendency was also observed for the other postures; while for passive THUMS V4, prescribed motion-based settling was generally associated with a larger head peak excursion than for a purely gravity-based case. The results showed an opposite trend for reactive THUMS V5.

4) Friction coefficient of the seat contact

The variation of the friction coefficient (0.3, 0.4, 0.5) between seat and pelvis of the HBM caused changes in the peak excursion of the Trochanter Major and therefore the head. However, not all postures were affected to the same extent. Posture D was practically unaffected by the variation of the friction coefficient, while posture A and posture AL showed more sensitivity regarding this parameter. The peak excursions of the head plotted over the peak excursions of the Trochanter Major are shown in Appendix F (Fig. F-1) for the five postures. The peak excursions of the hip were in the range of 24 to 42 mm for the passive THUMS V4 and between 9 to 24 mm for the reactive THUMS V5.

E. Effect of Combined Posture and Boundary Condition

The relative change in the peak head excursion caused by varying the boundary conditions was compared with the respective baseline simulation for each HBM posture. The results showed a generally higher sensitivity of reactive THUMS V5 (Fig. 8, a) than of passive THUMS V4 (Fig. 8, b) associated with the change of investigated boundary conditions. The trends between HBMs and between different postures, however, were comparable. The seat model had the greatest influence on both passive THUMS V4 and reactive THUMS V5.

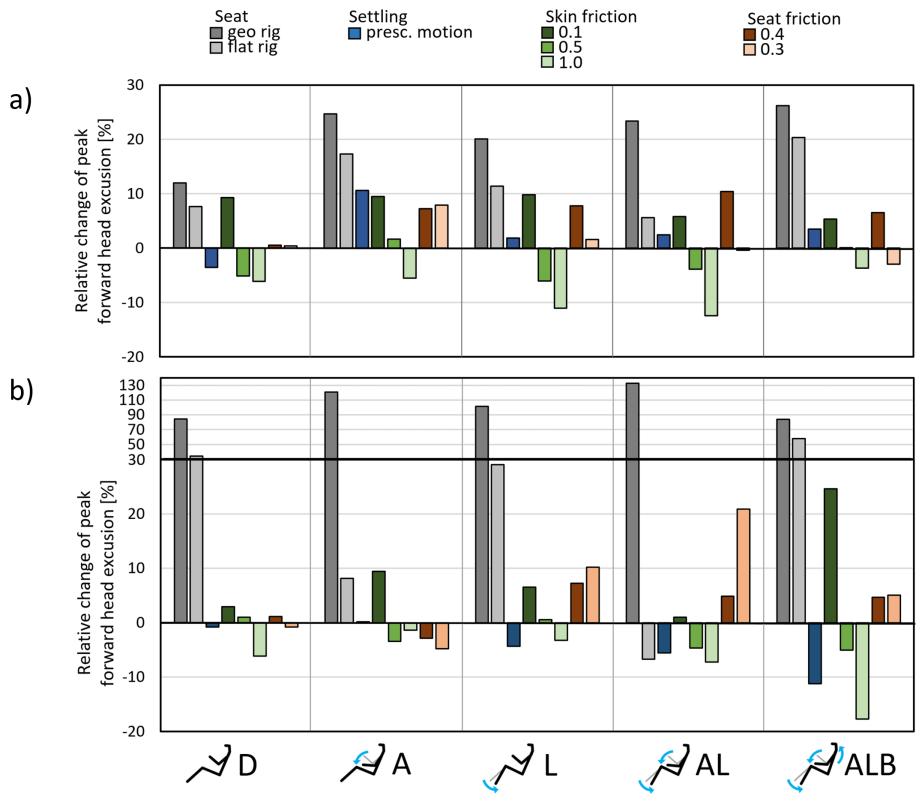

Fig. 8. Relative change of peak forward head excursion for the five postures due to parameter variation compared to baseline simulation of the respective posture (deformable seat, gravity settling, skin friction 0.3, seat friction 0.5) for passive THUMS V4 (a) and THUMS V5 (b).

For passive THUMS V4, changing the seat type (grey bars) had a notable influence on all postures. The geometric rigid seat (geo rig) and the flat rigid seat (flat rig) in particular increased the peak head excursion by approx. 10% to 25%. Prescribed motion settling (blue bars) showed a greater head excursion compared to the gravity settling method and showed a minor increase for almost all postures, except for posture D. Reducing the friction coefficient of the arms to thigh contact (green bars) to 0.1 showed a rising of the head excursion compared to the baseline friction coefficient (0.3), suggesting that load is transferred via the hands-thighs loading path. Corresponding to this trend a higher friction coefficient (0.5 and 1.0) decreased the peak head excursion. The influence of the friction coefficient of the HBM to seat contact (red bars) seemed to be very dependent on the posture. While posture D is nearly unaffected, other postures were affected by up to 10%.

Fig. 8 (b) shows the relative change of peak head excursion for the relaxed THUMS V5 caused by the variation of the boundary conditions of the simulation set-up for each posture (D, A, L, AL, ALB). Variation of the seat type (grey bars) had a remarkable influence on all postures. Switching the seat material to rigid (geo rig) caused about double the head excursion (+84% to +133%) compared to the baseline simulations. Prescribed motion settling (blue bars) showed an overall decrease of the peak head excursion (up to -11%). Variation of the skin friction coefficient in the range of 0.1 and 1.0 (green bars) caused changes in the range of -6% to +9%, only the posture ALB showed a greater sensitivity, which resulted in changes of -18% to +25%. Reducing the seat friction coefficient from 0.5 (baseline) to 0.3 and 0.4 resulted in relative changes between -5% and +10% of peak head excursion (red bars).

IV. Discussion

Experimental Volunteer Sled Tests

Simulations were set up based on volunteer tests with a backward mounted padded seat on an acceleration sled system, including six male participants close to 50th percentile anthropometry (Table I). The acceleration pulses were found to be close to actual AEB pulses (*Cluster 2* with and without contact) [45]. The acceleration pulse (T03) had a maximum of 0.47 g ([45]: 0.58 g (SD 0.15)), a ramp-time of 0.33 s ([45]: 0.71 s (SD 0.36), and a jerk of 1.15 g/s ([45]: 0.96 g (SD 0.47)) The peak forward head excursion showed highly subject-specific, however, variations between repeated tests for the same volunteer were comparably small suggesting viable repeatability of the test conditions. The notable subject-specific differences observed in the volunteer study are assumed to be caused by multiple factors: A state of awareness probably existed among some volunteers in this context due to explicit boundary conditions and preparation work, although the exact onset of the acceleration was not indicated. This was also indicated by active neck muscles at acceleration onset for some of the volunteers. The awareness of the volunteer and acclimation caused by repeated tests were shown to influence volunteer behaviour [24, 35, 46–47]. One of the six volunteers was thus selected for the conducted simulation study. Based on literature data [32, 34], the peak head excursion of volunteer P03 was within the range of the reported average values for comparable test setups. Furthermore, no pre-tensed muscles were observed by EMG measurements for the specific volunteer. For the subject-specific test replication, the posture of the HBM and the acceleration pulse of volunteer P03 rather than averaged data was used. Test 01 of the volunteer was not included within this study in detail, as the peak excursions were comparable to Test 03 with a maximum deviation of all landmarks below 10 mm. Peak forward excursions of the head of volunteer P03 (204 mm, 209 mm and 276 mm) were comparable to averaged data of sled tests below 1 g acceleration including male volunteers in the passenger posture with an initial relaxed muscle state. Approx. 250 mm at a half-sinus shaped acceleration pulse with a peak of 0.82 g with a standard seatbelt [34] and approx. 330 mm at 0.6 g with a lap belt and arms not resting on their laps, but hanging at their sides [32] was found in previous studies.

Volunteer P03 found his hands slipping on the thighs during Test 02, while probably having the intention of supporting the torso subjected to forward movement by inertial force. However, relative motion between the hands and the thighs was limited to elastic deformation of soft tissue and no longitudinal relative motion was observed in Test 01 and Test 03. Since the target attached to the anatomical landmark on the wrist was partly covered by the thigh at the time of peak excursion, visual target tracking was adjusted manually. Reference [22] concluded from braking events in a passenger car that the legs are most important for limiting the forward movement of volunteers. However, movement of this kind relative to the seat of the whole body was not observed in the volunteer study that was chosen for this research. During the full braking events in a passenger car examined by [29] the muscle activity of the upper extremities only had a minor influence on the excursion of

the volunteers. EMG data showed muscle activity in the upper extremities below 3% maximum voluntary contraction (MVC), whereas neck and lumbar muscles had the highest activity influencing the forward movement.

HBM simulations

The simulation results suggest that correct arm posture on the thighs is more important than the HBM's leg posture, in order to show a comparable head excursion in the volunteer test. Adjusting the leg posture only had a minor effect, which similarly impacted all included HBMs and was independent of muscle activation. Therefore, torso support via the arm-thighs load path seemed to be crucial for the head excursion. The back posture had a notable influence as it increased the relative motion between thighs and the arms and therefore increased the head excursion. Since the adaptation of the muscle models of the active HBMs was not within the scope of this study, simulations with varying friction coefficients were run in order to determine whether this behaviour could be thereby influenced. Thus, also high and low coefficients out of realistic bounds, were included in order to cover a wide range for the influence of the hands to thighs interaction. Gravity based settling, in order to reach the equilibrium of forces in direction of gravity, showed robust results in this study, as only very slight additional settling movement of the HBMs was observed after t_0. The prescribed motion-based settling led to an additional settling movement of the head and neck region after the actual settling process (first 0.2 s of the simulation), which also influenced the forward excursion to a different extent depending on posture and HBM. Moreover, the pressure distribution on the seat (seat and back surface) was compared to the HBMs results. The visual comparison (Appendix D, Fig. D-1) between volunteer P03 and passive THUMS V4 appeared to be more closely comparable to volunteer P03 than passive THUMS V5. Furthermore, the results suggested that the modelling of a deformable seat with respect to both material properties and realistic geometry is an important issue. The correlation between peak excursions of head and Trochanter Major proved to be fairly linear for the reactive THUMS V5, while the results for passive THUMS V4 showed more variation. Considering a non-deformable material by switching the seat to rigid or using a simple flat and rigid seat increased the head excursions of the HBM remarkably. As the simulations revealed a relatively strong influence of the seat model on the head excursion, further work was done for calibration of the seat model. Data on the mechanical stiffness of the seat was measured via tests with hemispheric impactors (ø150 mm and ø250 mm) mounted on a hydraulic cylinder. Force-displacement curves of indentation tests for different locations were derived (shown in Appendix G, Fig. G-1). During the calibration process, adaptation of the material parameters of the leather skin and the spring definitions under the seat, were found to be necessary. Moreover, the oscillations in force-deflection curves of the original seat model (mainly seat structure frontal in Fig G-3), were addressed by adding beam elements (MAT_Damper_Viscous), coincident to the existing nonlinear elastic beam elements (representing stiffness of the mounting structure). The foam material remained unchanged, as it had already been calibrated. Overall, a comparable response between simulations and tests was observed, as shown in Appendix G (Fig. G-2 and Fig. G-3). Ultimately, the extensively calibrated seat model was publicly released on the OpenVT platform [37].

Limitations

Several limitations are inherent in the simulations and are therefore discussed. First of all, the results may only be valid for an acceleration pulse comparable to the pulse utilised for this study and for purely longitudinal loadings. The transferability for other pre-crash acceleration pulses should thus be considered in detail for each case, as there can be notable differences between acceleration levels and durations. Furthermore, a statement about the transferability of the results to oblique and lateral accelerations cannot be made. Moreover, the postures of the HBMs did not meet the volunteer angles precisely, which may be caused by anthropometrical differences. In addition, the ankle position was not adjusted, although the volunteer tests were conducted with the feet placed flat on the footrest. No relative motion between the footrest and the feet was observed either in the volunteer tests or the simulations. A seat model with a constant upright backrest angle only was used for all tests and simulations. Therefore, the results may have limited validity for deviating seated positions, e.g., novel seated postures with a more reclined seatback. Anthropometrical differences were addressed to define the target posture by the utilised positioning tool but no adaptions to the HBMs, e.g., scaling or morphing, were made, although such techniques were shown to contribute to increased biofidelity for specific anthropometries [48–49]. Posture changes of HBMs are associated with changes in mesh quality and simulation time [50] and changes in response [51]. However, these influences were not considered in detail within the scope of this study.

The PID gains of the muscle of the utilised active HBM model have been calibrated to volunteer responses from higher acceleration pulses compared to the pulse used for this study by the original HBM developers [10–11, 17–19]. However, the observed excursions were in agreement with the volunteer P03 selected as reference.

Moreover, it seems likely that the inertia of the arms in the driver posture also contributed to excursions of the HBMs in related postures. In particular, the inertia effects and load path effects of the arms were not investigated separately. This could be done in future by disabling the contact between arms and thighs, which would however lead to unrealistic kinematics of the arms. The evaluation of relative movement of the wrists on the thighs for the postures with positioned arms (A, AL, ALB) suggested a remarkable contribution to the torso support. The muscle activation levels of the active HBMs were not evaluated and compared to volunteer results. This was due to the fact that EMG data was not obtained for the upper extremities as they were assumed to have only a minor effect when planning the tests.

Several parameters were identified in the simulation study as influencing the peak head excursion of the included HBMs. The findings of this study may not be representative for volunteer tests, as it is not clear if the same factors that drove the HBM response would also have driven the volunteer response. Nevertheless, some of these parameters may be included in future volunteer studies and will thus allow investigation of impact on volunteer response.

Outlook

A detailed level of documentation, e.g., posture, trajectories, boundary conditions, is clearly beneficial for the replication of volunteer tests with HBMs. The results of this study suggest that detailed data, e.g., volunteer posture documentation and characterisation of seat model, are vital for HBM simulations of low severity events such as braking manoeuvres. Further test data from volunteer tests would be an important step towards gaining more detailed insight into the contribution of the upper extremities to support the torso. For example, a pressure measuring mat could be placed on the thighs in order to measure the force transmitted. Muscle activity of active HBMs may also be compared to the volunteer results, including those for the upper extremities. Moreover, future tests with volunteers may include different arm postures relevant for occupants of automated cars, e.g., reading a book or using a smartphone. The utilisation of a production seat or a padded seat in volunteer tests, may also be relevant as a means of mimicking the boundary conditions of a passenger car as this was a major influence on HBM response. Too detailed seat models are however difficult to replicate and need extensive calibration and validation efforts. Generic seats with deformable foams in the stiffness range of production seats might therefore be a good trade-off between realistic interaction and well-described boundary conditions.

V. CONCLUSIONS

The effect of varying boundary conditions and initial postures during low-severity loadings representing a braking manoeuvre was investigated using different passive and reactive HBMs. Simulation results suggest that the posture of the HBM is a major influence, as it had a strong effect on the head excursions (approx. -25% to -80% relative change compared to the baseline posture). Furthermore, it was found in particular that the position of the wrists on the thighs is of great importance for replicating the behaviour observed in the volunteer tests with the HBMs, where no steering wheel was available. The findings of this study should be further investigated in volunteer tests to analyse the effect of initial postures on human responses. Head excursions were also highly affected by the compliance of the seat model, highlighting the importance of the seat modelling. Gravity-based settling showed the best results for simulations with low-severity pulses.

The dataset of the volunteer tests and seat model used in this study have been made publicly available. The volunteer tests were performed in a simplified, well-described environment and the current study has shown that they are useful for the evaluation of HBM responses. The tests could thus be used for validation of active HBMs in a step-wise approach, starting with a low complexity level.

VI. ACKNOWLEDGEMENT

This study received funding from the European Union Horizon 2020 Research and Innovation Programme under Grant Agreement No. 768947 (OSCCAR). The document reflects only the author’s view and the Commission is not responsible for any use that may be made of the information it contains.

The authors gratefully acknowledge the use of high-performance computing resources provided by the ZID (Zentraler Informatikdienst) at Graz University of Technology (Graz, Austria).

The authors would like to acknowledge financial support for the volunteer tests from the "COMET K2 - Competence Centers for Excellent Technologies Program" of the Austrian Federal Ministry for Transport, Innovation and Technology (bmvit), the Austrian Federal Ministry of Science, Research and Economy (bmwfw), the Austrian Research Promotion Agency (FFG), the Province of Styria and the Styrian Business Promotion Agency (SFG).

VII. References

1. Scanlon JM, Kusano KD, Gabler HC. (2015) Analysis of Driver Evasive Maneuvering Prior to Intersection Crashes Using Event Data Recorders. Traffic Injury Prevention. Issue sup2: Peer-Reviewed Journal for the 59th Annual Scientific Conference of the Association for the Advancement of Automotive Medicine (AAAM), October 2015.
2. Ejima S, Ito D, Satou F, Mikami K, Ono K, Kaneoka K *et al.* (2012) Effects of pre-impact swerving/steering on physical motion of the volunteer in the low-speed side-impact sled test. Proceedings of IRCOBI Conference, 2012, Dublin, Ireland.
3. Ejima S, Zama Y, Ono K, Kaneoka K, Shiina I, Asada H. (2009) Prediction of Pre-impact Occupant Kinematic Behavior Based on the Muscle Activity during Frontal Collision. Proc. of 21st ESV Conference.
4. Official Journal of the European Union. "Regulation (EU) 2019/2144", https://eur-lex.europa.eu/eli/reg/2019/2144/oj.
5. Yamada K, Gotoh M, Kitagawa Y, Yasuki T (2016) Simulation of Occupant Posture Change during Autonomous Emergency Braking and Occupant Kinematics in Frontal Collision. *Proceedings of IRCOBI Conference,* 2016, Malaga, Spain.
6. Schoeneburg R, Baumann K-H, Fehring M. (2011) The Efficiency of PRE-SAFE Systems in Pre-braked Frontal Collision Situations. Proceedings of the 22nd ESV Conference; Washington, D.C.,
7. Beeman SM, Kemper AR, Madigan ML, Franck CT, Loftus SC. (2012) Occupant kinematics in low-speed frontal sled tests: Human volunteers, Hybrid III ATD, and PMHS. Accident Analysis & Prevention, 47: pp.128–139.
8. Klug C, Feist F, Schneider B, Sinz W, Ellway J, van Ratingen M (2019) Development of a Certification Procedure for Numerical Pedestrian Models*. Proceedings of International Technical Conference on the Enhanced Safety of Vehicles,* 2019, Eindhoven, Netherlands.
9. Iwamoto M, Nakahira Y, Kimpara H, Sugiyama T, Min K. (2012) Development of a Human Body Finite Element Model with Multiple Muscles and their Controller for Estimating Occupant Motions and Impact Responses in Frontal Crash Situation. Stapp Car Crash Journal, Vol. 56.
10. Kato D, Nakahira Y, Iwamoto M. (2017) A study of muscle control with two feedback controls for posture and reaction force for more accurate prediction of occupant kinematics in low-speed frontal impacts, 25th ESV.
11. Kato D, Nakahira A, Atsumi N, Iwamoto M. (2018) Development of Human-Body Model THUMS Version 6 containing Muscle Controllers and Application to Injury Analysis in Frontal Collision after Brake Deceleration. Proceedings of IRCOBI Conference, 2018, Athens, Greece.
12. Iwamoto M, Nakahira Y. (2015) Development and Validation of the Total HUman Model for Safety (THUMS) Version 5 Containing Multiple 1D Muscles for Estimating Occupant Motions with Muscle Activation During Side Impacts. Stapp Car Crash Journal, Vol. 59.
13. Östh J, Eliasson E, Happee R, Brolin K. (2014) A method to model anticipatory postural control in driver braking events. Gait & posture, 40(4): pp.664–669.
14. Correia MA, McLachlin SD, Cronin DS. (2020) Optimization of muscle activation schemes in a finite element neck model simulating volunteer frontal impact scenarios. Journal of biomechanics, 104: p.109754.
15. Martynenko OV, Wochner I, Nölle LV, Alfaro EH, Schmitt S, Mayer C *et al.* (2021) Comparison of the Head-Neck Kinematics of Different Active Human Body Models with Experimental Data. Proceedings of IRCOBI Conference, 2021, online.
16. Beeman SM, Kemper AR, Madigan ML, Duma SM. (2011) Effects of bracing on human kinematics in low-speed frontal sled tests. Annals of Biomedical Engineering, 39(12): pp.2998–3010.
17. Toyota Motor Corporation, Toyota Central R&D Labs., Inc. (2019) THUMS Documentation - Total Human Model for Safety (THUMS) AM50 Occupant Model 5.03.
18. Toyota Motor Corporation, Toyota Central R&D Labs., Inc. (2019) THUMS Documentation - Total Human Model for Safety (THUMS) AM50 Occupant Model 6.02.
19. Kato D, Nakahira Y, Iwamoto M. (2017) Development of a muscle controller for prediction of occupant kinematics in consideration of muscle tone conditions. Jstage.
20. Kitagawa Y, Yasuki T. (2014) Development and Application of THUMS Version 4. 5th International Symposium: “Human Modeling and Simulation in Automotive Engineering”.
21. Schneider LW, Robbins DH, Pflüg, M.A., Snyder, R.G. (1983) Anthropometry of Motor Vehicle Occupants: Procedures, summary findings and appendices. The University of Michigan - Transportation Research Institute.

22. Morris R, Cross G. (2005) Improved Understanding of Passenger Behaviour During Pre-Impact Events to Aid Smart Restraint Development. Proceedings of the 19th International Technical Conference on the Enhanced Safety of Vehicles (ESV), Washington DC.
23. Kümpfbeck M, Oertel D, Pilatur K. (1999) Occupant kinematics during emergency braking. Proceedings of IRCOBI Conference, 1999, Sitges, Spain.
24. Reed M, Ebert S, Park BK, Jones M. (2018) Passenger Kinematics During Crash Avoidance Maneuvers. University of Michigan Transportation Research Institute Final Report. UMTRI-2018-5.
25. Huber P, Kirschbichler S, Prüggler A, Steidl T. (2015) Passenger kinematics in braking, lane change and oblique driving maneuvers. Proceedings of IRCOBI Conference, 2015, Lyon, France: pp.783–802.
26. Huber P, Kirschbichler S, Prüggler A, Steidl T. (2014) Three-Dimensional Occupant Kinematics During Frontal, Lateral and Combined Emergency Maneuvers. Proceedings of IRCOBI Conference, 2014, Berlin, Germany.
27. Kirschbichler S, Huber P, Prüggler A, Steidl T, Sinz W, Mayer C *et al.* (2014) Factors Influencing Occupant Kinematics during Braking and Lane Change Maneuvers in a Passenger Vehicle. Proceedings of IRCOBI Conference, 2014, Berlin, Germany.
28. Östh J, Ólafsdóttir JM, Davidsson J, Brolin K. (2013) Driver Kinematic and Muscle Responses in Braking Events with Standardand Reversible Pre-tensioned Restraints: Validation Data for Human Models. Stapp Car Crash Journal, 57: pp.1–41.
29. Olafsdottir J, Östh J, Davidsson J, Brolin K. (2013) Passenger Kinematics and Muscle Responses in Autonomous Braking Events with Standard and Reversible Pre-tensioned Restraints. Proceedings of IRCOBI Conference, 2013, Gothenburg, Sweden.
30. Carlsson S, Davidsson J. (2011) Volunteer occupant kinematics during driver initiated and autonomous braking when driving in real traffic environments. Proceedings of IRCOBI Conference, 2011, Krakow, Poland.
31. Behr M, Poumarat G, Serre T, Arnoux P-J, Thollon L, Brunet C. (2010) Posture and muscular behaviour in emergency braking: an experimental approach. Accident; analysis and prevention, 42(3): pp.797–801.
32. Ejima S, Koshiro O, Holcombe S, Kaneoka K, Fukushima M. (2007) A Study on Occupant Kinematic Behaviour and Muscle Activities during Pre-Impact Braking Based on Volunteer Tests. Proceedings of IRCOBI Conference, 2007, Maastricht, The Netherlands.
33. Ejima S, Zama Y, Satou F, Holcombe S, Ono K, Kaneoka K *et al.* (2008) Prediction of the Physical Motion on Human Body based on Muscle Activities during Pre-Impact Breaking. Proceedings of IRCOBI Conference, 2008, Bern, Switzerland.
34. Ito D, Ejima S, Kitajima S, Katoh R, Ito H, Sakane M *et al.* (2013) Occupant Kinematic Behavior and Effects of a Motorized Seatbelt on Occupant Restraint of Human Volunteers during Low Speed Frontal Impact: Mini-sled Tests with Mass Production Car Seat. Proceedings of IRCOBI Conference, 2013, Gothenburg, Sweden.
35. Chan H, Albert D, Gayzik FS, Kemper AR. (2021) Assessment of Acclimation of 5th Percentile Female and 50th Percentile Male Volunteer Kinematics in Low-Speed Frontal and Frontal-Oblique Sled Tests. SAE International Journal of Transportation Safety, 9(1): pp.3–103.
36. Kirschbichler S, Klein C, Klug C, Kofler D. "Precooni & OM4IS Data", https://zenodo.org/record/5747370.
37. Kofler D, Heider E, Klug C, Erlinger N, Mishra A, Ghosh P. "PRECOONI-OM4IS Precrash seat model", https://openvt.eu/osccar/precrash_seat_models/precooni-om4is [Accessed 14 February 2022].
38. Pucher J. "OSCCAR Positioning", https://openvt.eu/osccar/positioning/positioning [Accessed 3 May 2022].
39. Schachner M, Micorek J, Luttenberger P, Greiml R, Klug C, Rajinovic S. "Dynasaur - Dynamic simulation analysis of numerical results", https://gitlab.com/VSI-TUGraz/Dynasaur.
40. Toyota. "Thums user policy", https://www.toyota.co.jp/thums/contents/pdf/THUMS_USER_POLICY.pdf [Accessed 3 March 2021].
41. Klein C, Gonzales-Garcia M, Weber J, Bosma F, Lancashire R, Breitfuss D *et al.* (2021) A Method for Reproducible Landmark-based Positioning of Multibody and Finite Element Human Models. Proceedings of IRCOBI Conference, 2021, online.
42. Eliasson E, Wass J. (2015) Industrialisation of a Finite Element Active Human Body Model for Vehicle Crash Simulations. Master Thesis CHALMERS UNIVERSITY OF TECHNOLOGY.
43. Larsson E, Iraeus J, Fice J, Pipkorn B, Jakobsson L, Brynskog E *et al.* (2019) Active Human Body Model Predictions Compared to Volunteer Response in Experiments with Braking, Lane Change, and Combined Manoeuvres. Proceedings of IRCOBI Conference, 2019, Florence, Italy.
44. PIPER Project. "PIPER Project", http://www.piper-project.eu [Accessed 2 May 2022].
45. Graci V, Maltenfort M, Schneider M, Griffith M, Seacrist T, Arbogast KB. (2021) Quantitative characterization of AEB pulses across the modern fleet. Traffic injury prevention, 22sup1S62-S67.

46. Blouin J-S, Descarreaux M, Bélanger-Gravel A, Simoneau M, Teasdale N. (2003) Attenuation of human neck muscle activity following repeated imposed trunk-forward linear acceleration. Experimental brain research, 150(4): pp.458–464.
47. Muehlbauer J, Gonzales-Garcia M, Siebler L, Schick S, Peldschus S. (2020) Evaluation of initial volunteer test conditions in locally focused validation experiments for active human body models. IRCOBI conference 2020.
48. Piqueras-Lorente A, Iraeus J, Lorente A, Lopez-Valdes F, Juste-Lorente O, Maza-Frechin M *et al.* (2018) Kinematic Assessment of Subject Personification of Human Body Models (THUMS). Proceedings of IRCOBI Conference, 2018, Athens, Greece.
49. Hwang E, Hu J, Reed MP. (2020) Validating diverse human body models against side impact tests with post-mortem human subjects. Journal of biomechanics, 98: p.109444.
50. Costa C, Caffrey J, Kleek B von, Weaver A, Hallman J, Akima S *et al.* (2021) Effect of Postural Adjustment Methods on Mesh Quality & Simulation Time of Human Body Models. Proceedings of IRCOBI Conference, 2021, online.
51. Ando T, Kitagawa Y, Eggers A. (2019) Influence of Posture Adjustment Methods for Human Body Models on Injury Prediction. Proceedings of IRCOBI Conference, 2019, Florence, Italy.

APPENDIX A

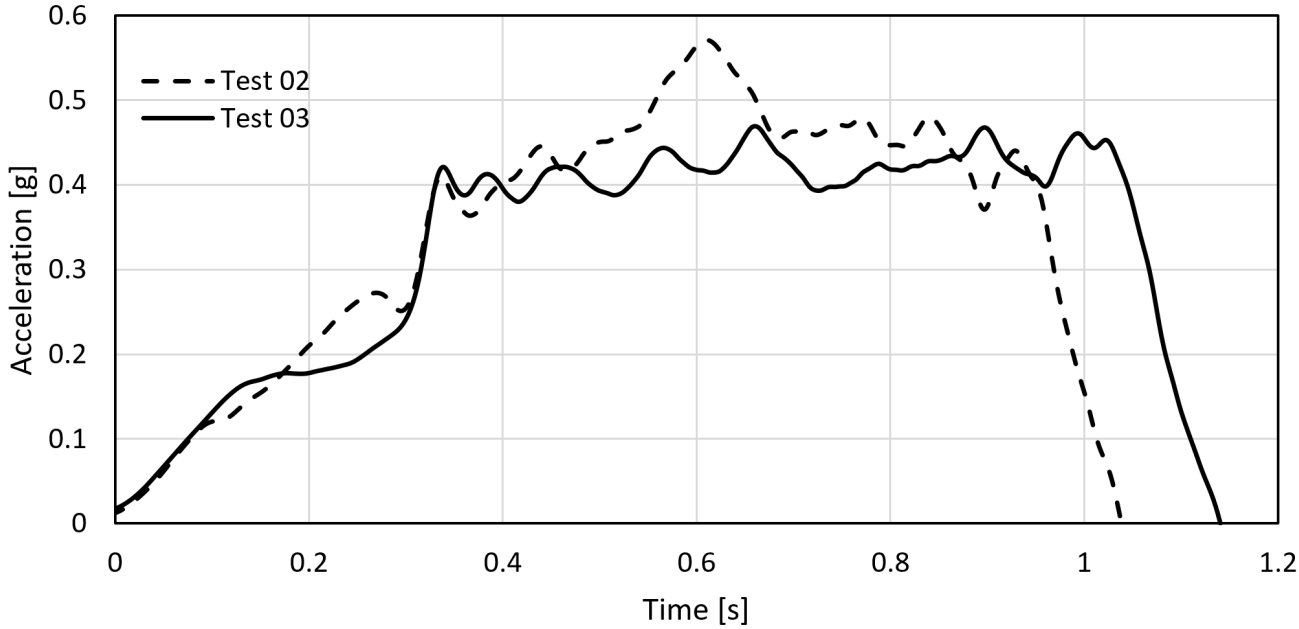

Fig. A-1. Sled acceleration over time for tests including volunteer P03, Test 03 was prescribed in simulations.

TABLE A-I
INITIAL VOLUNTEER LANDMARK COORDINATES FROM TEST 03 OF VOLUNTEER P03

Landmark	Name	x-coordinate [mm]	z-coordinate [mm]
ASL	Lateral malleolus	197.7	-47.5
CS	C5 vertebra	-568.8	-787.5
ELSL	Lateral epicondyle of humerus	-418.9	-461.7
HA	Upper margin of auditory canal	-572.1	-898.3
HO	Marker on sunglass	-497.8	-912.0
KSL	Lateral femoral epicondyle	3.2	-419.5
SHSL	Uppermost point of humerus	-565.0	-707.2
WRSL	Styloid process of ulna	-185.3	-473.6
TM	Trochanter major	-375.5	-261.6

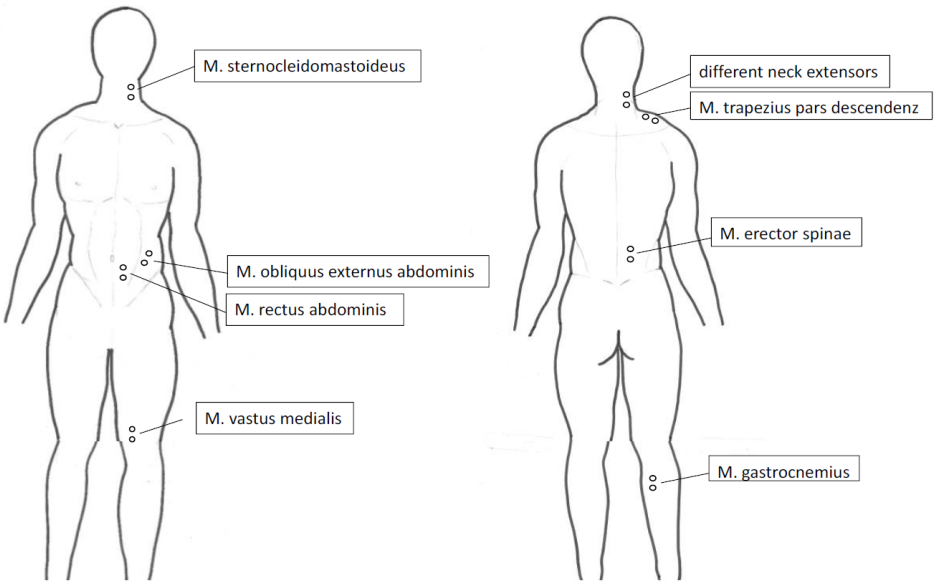

Fig. A-2. Electrode positions of surface EMG in anterior (left) and posterior (right) view.

APPENDIX B

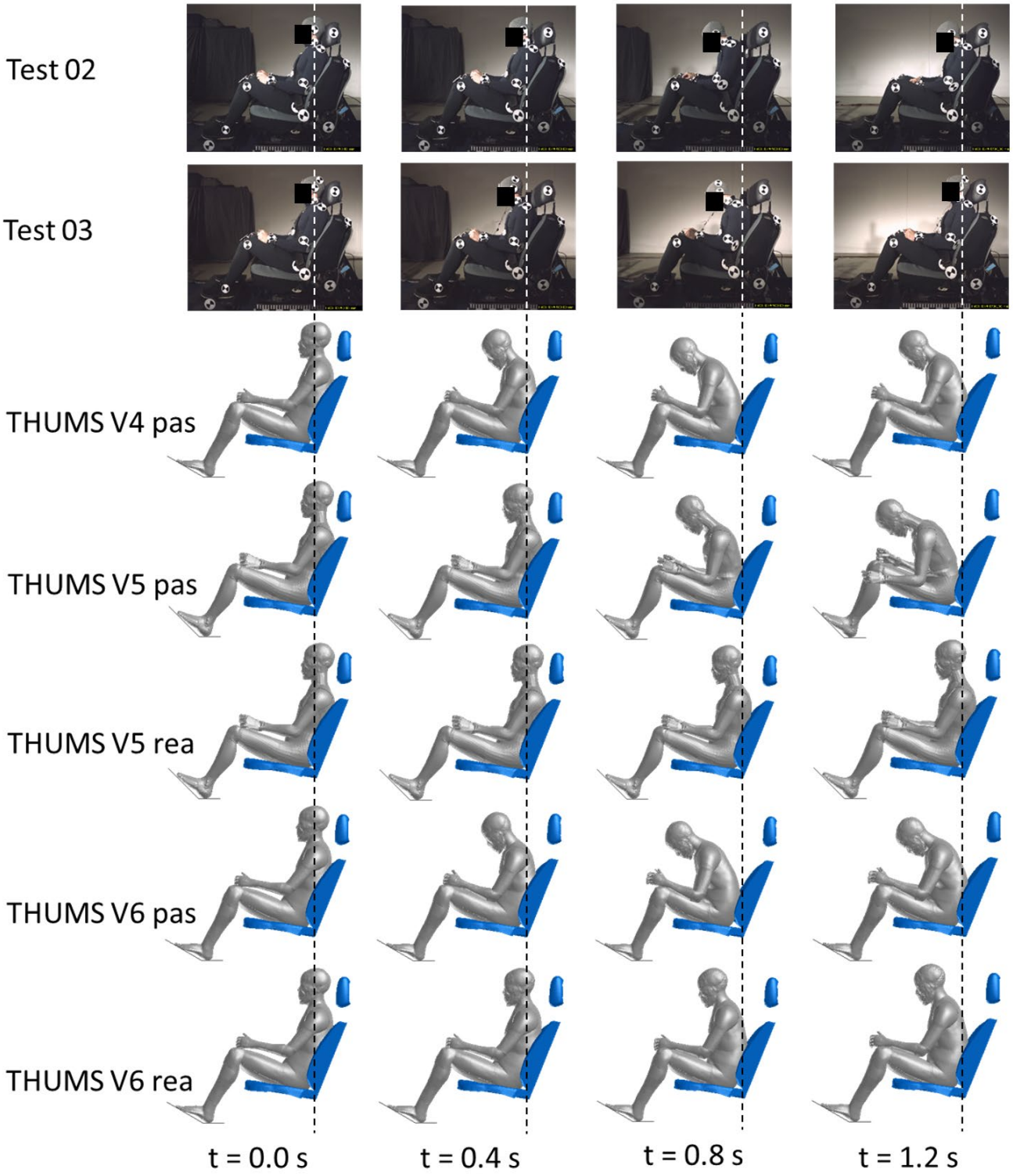

Fig. B-1. Images of the volunteer test and screenshots of simulations the HBMs in ALB posture at four time-steps (0.0 s, 0.4 s, 0.8 s, 1.2 s).

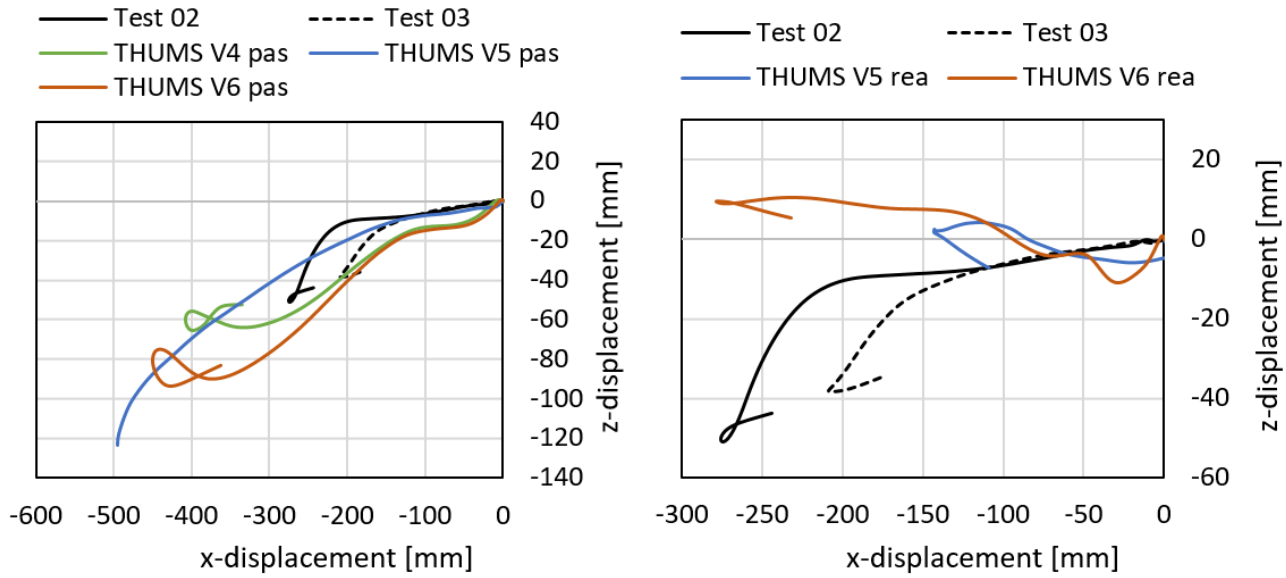

Fig. B-2. Head trajectories of passive HBMs (left) and active HBMs (right) in ALB posture compared to the volunteer response from P03 (Test 02 and Test 03).

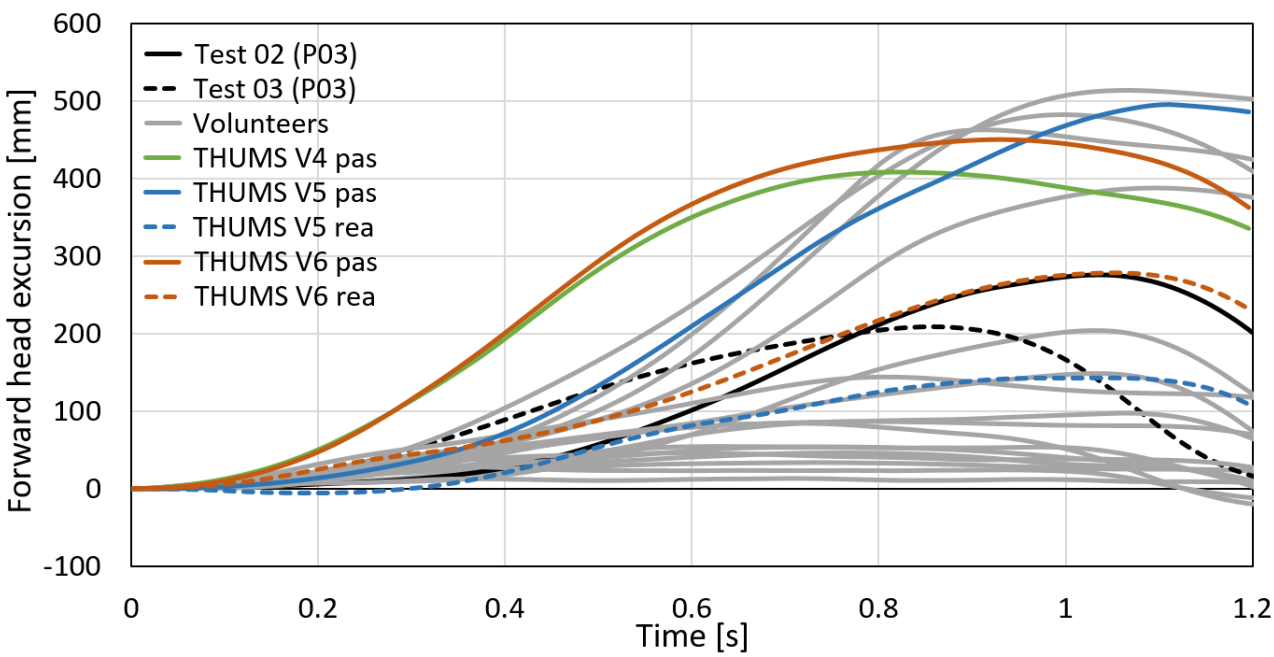

Fig. B-3. Forward excursion of the head over time of HBM simulations and including all volunteer responses of the experimental study.

TABLE B-I
PEAK FORWARD HEAD EXCURSION FOR DIFFERENT POSTURES FOR HBMS

THUMS / Posture	O [mm]	A [mm]	L [mm]	AL [mm]	ALS [mm]
Passive THUMS V4	543	418	494	403	408
Passive THUMS V5	476	255	437	350	496
Relaxed THUMS V5	195	77	172	69	143
Passive THUMS V6	593	453	522	429	450
Reactive THUMS V6	386	157	335	76	278

APPENDIX C

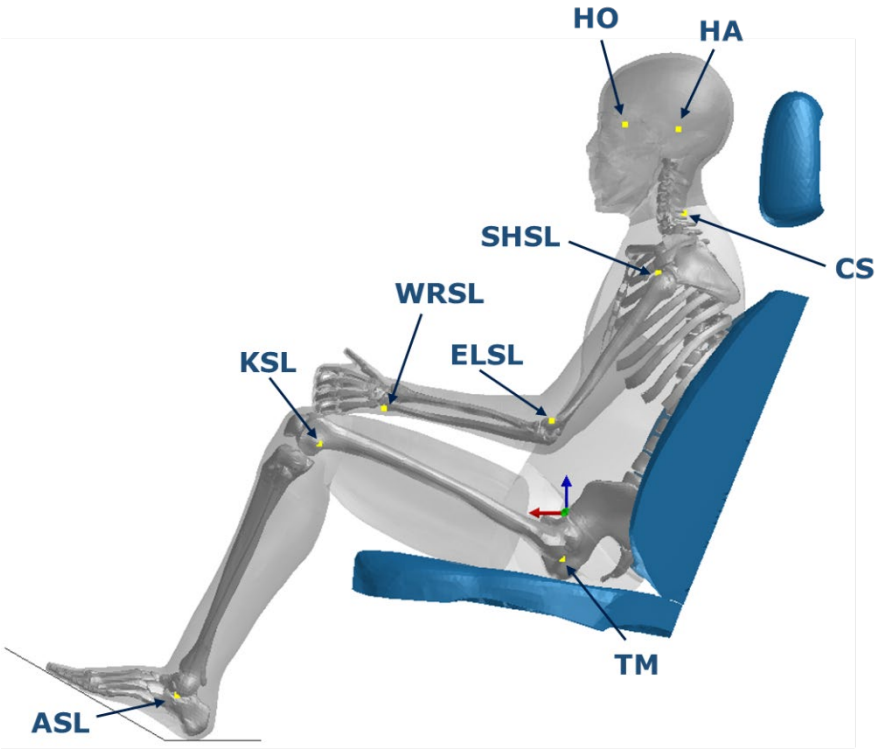

Fig. C-1. Overview of the anatomical landmarks of the volunteer test defined by nodes on cortical bones of the HBM (THUMS V4).

TABLE C-I
NODE IDS OF THE HBMS USED FOR DEFINITION OF ANATOMICAL LANDMARKS OF VOLUNTEER TEST

Landmark	Name	Node ID THUMS V4/V6	Node ID THUMS V5
ASL	Lateral malleolus	82001960	8230226
CS	C5 vertebra	89000576	8711148
ELSL	Lateral epicondyle of humerus	86006116	8641398
HA	Upper margin of auditory canal	88255707	8813682
HO	Marker on sunglass	88175683	8811920
KSL	Lateral femoral epicondyle	82072234	8250715
SHSL	Uppermost point of humerus	86007060	8641158
WRSL	Styloid process of ulna	86002476	8630257
TM	Trochanter major	82103360	8253877

APPENDIX D

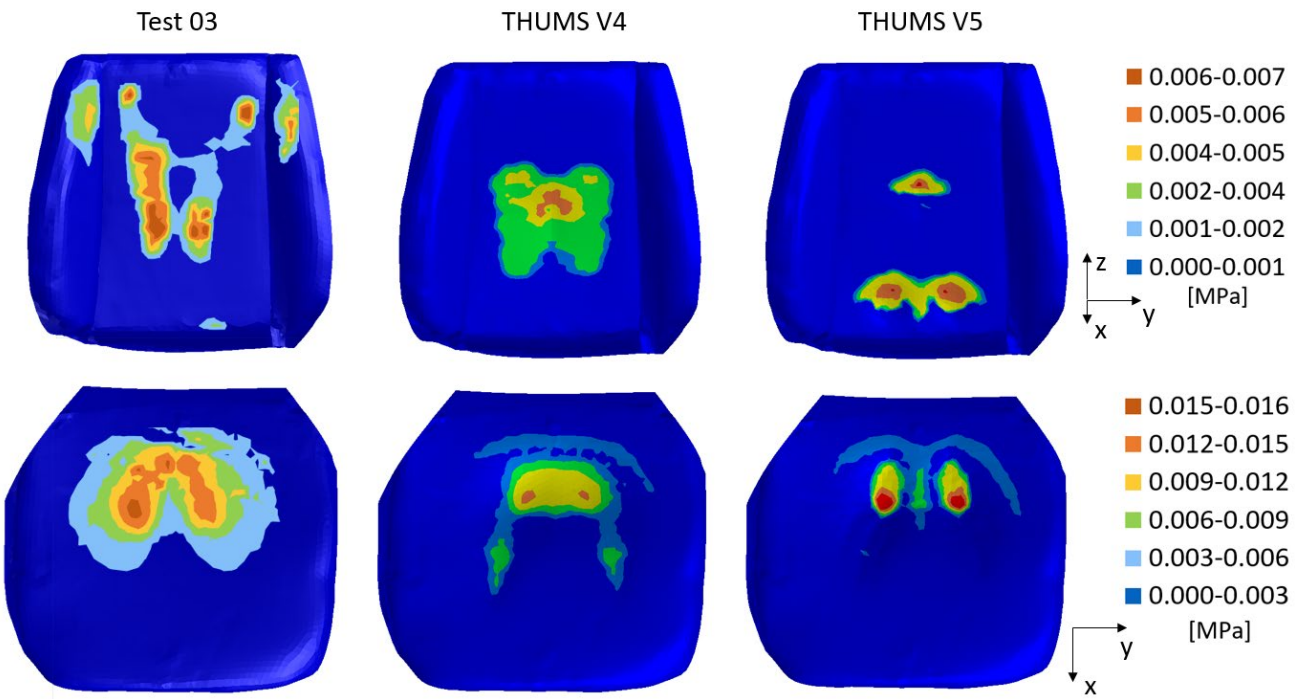

Fig. D-1. Seat pressure distribution from volunteer (P03, Test 03) (left), passive THUMS V4 (middle) and passive THUMS V5 (right) at stationary seated and after settling respectively. Note the different pressure ranges for colour shading of backrest and seat.

APPENDIX E

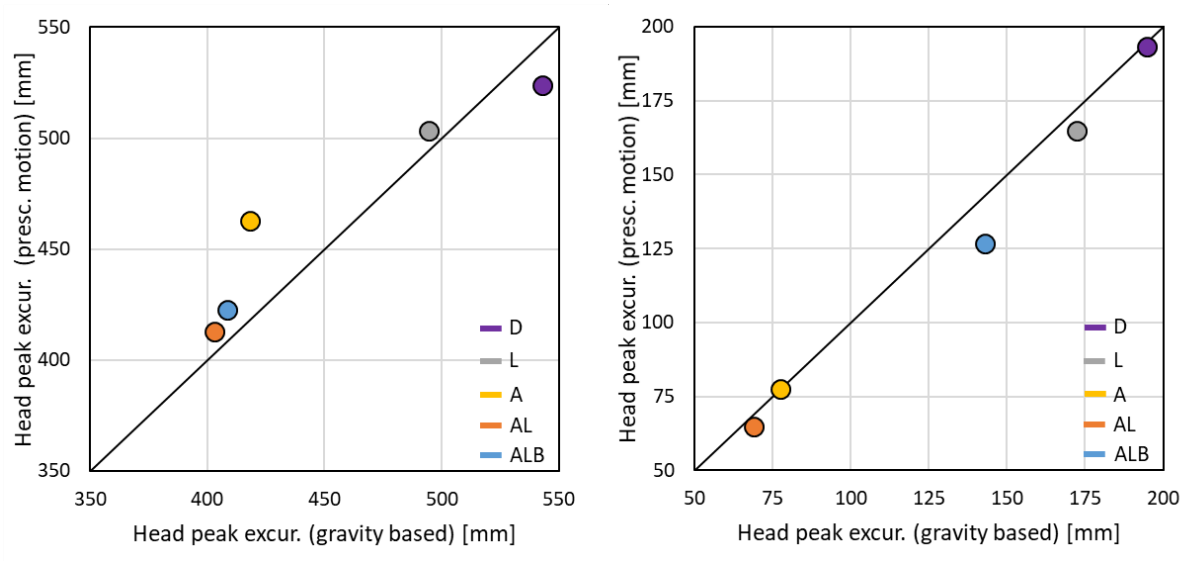

Fig. E-1. Cross-plots of peak excursions of landmark head for prescribed motion settling (ordinate) and gravity-based settling (abscissa) for passive THUMS V4 (left) and reactive THUMS V5 (right).

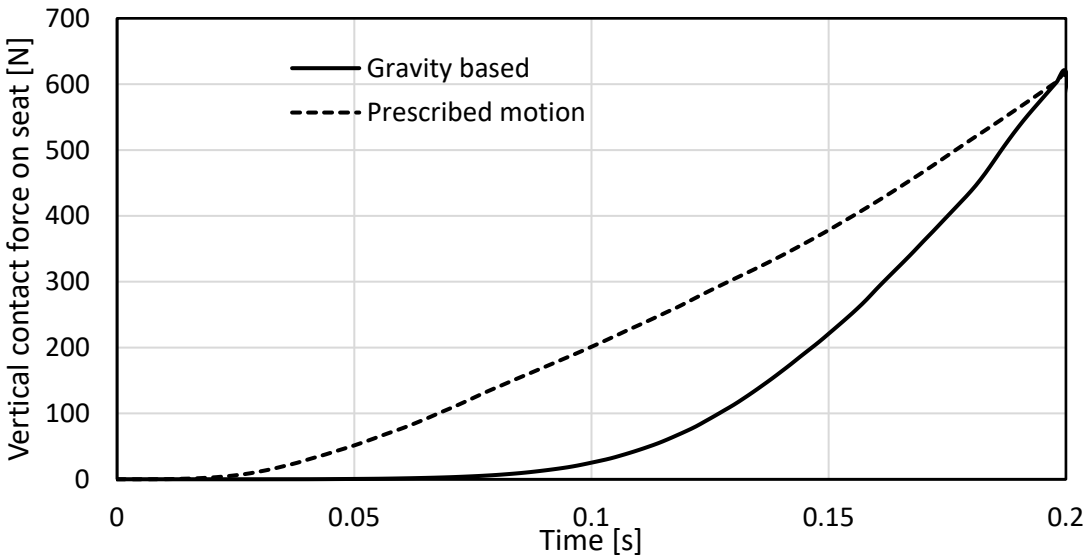

Fig. E-2. Vertical contact force on the seat over time during settling phase for prescribed motion settling and gravity-based settling of passive THUMS V4.

APPENDIX F

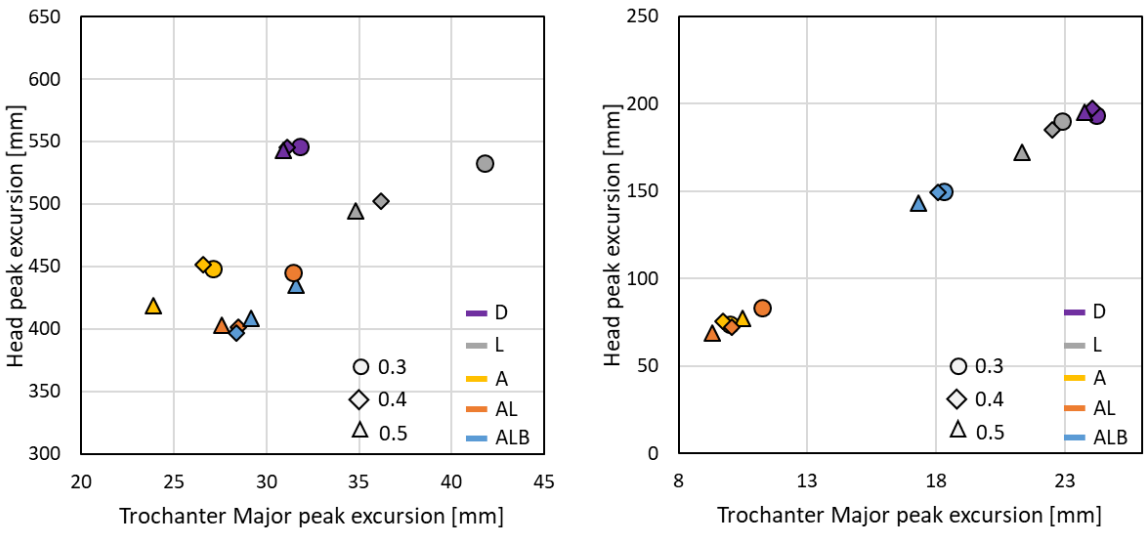

Fig. F-1. Cross-plots of peak excursions of landmarks head und Trochanter Major for seat friction coefficients (0.3, 0.4, 0.5) and postures (D, L, A, AL, ALB) for passive THUMS V4 (left) and reactive THUMS V5 (right).

APPENDIX G

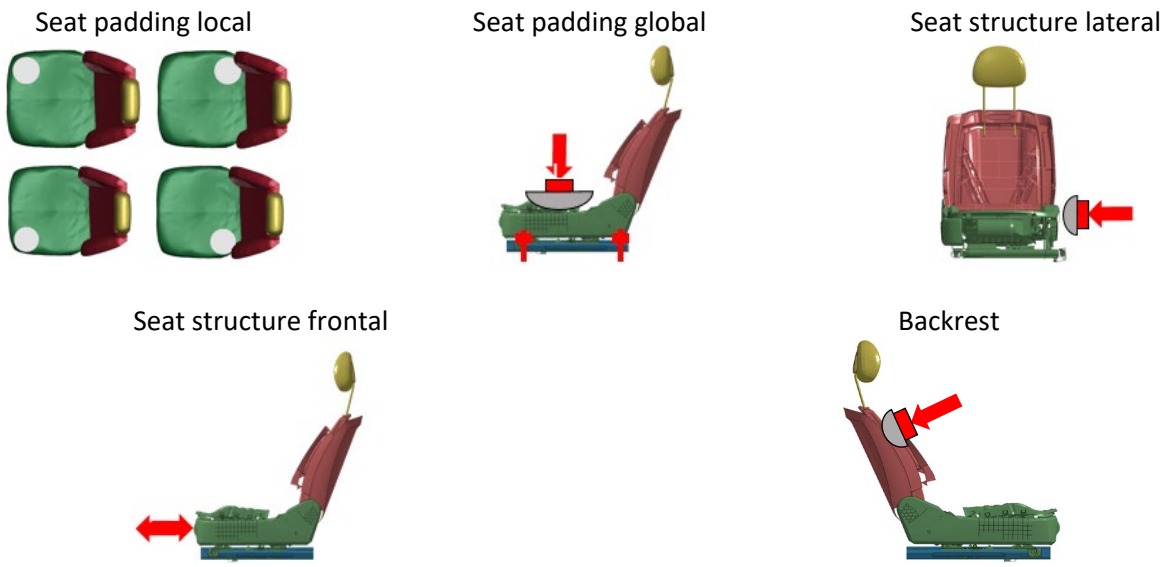

Fig. G-1. Overview of impactor test configurations for the seat model calibration.

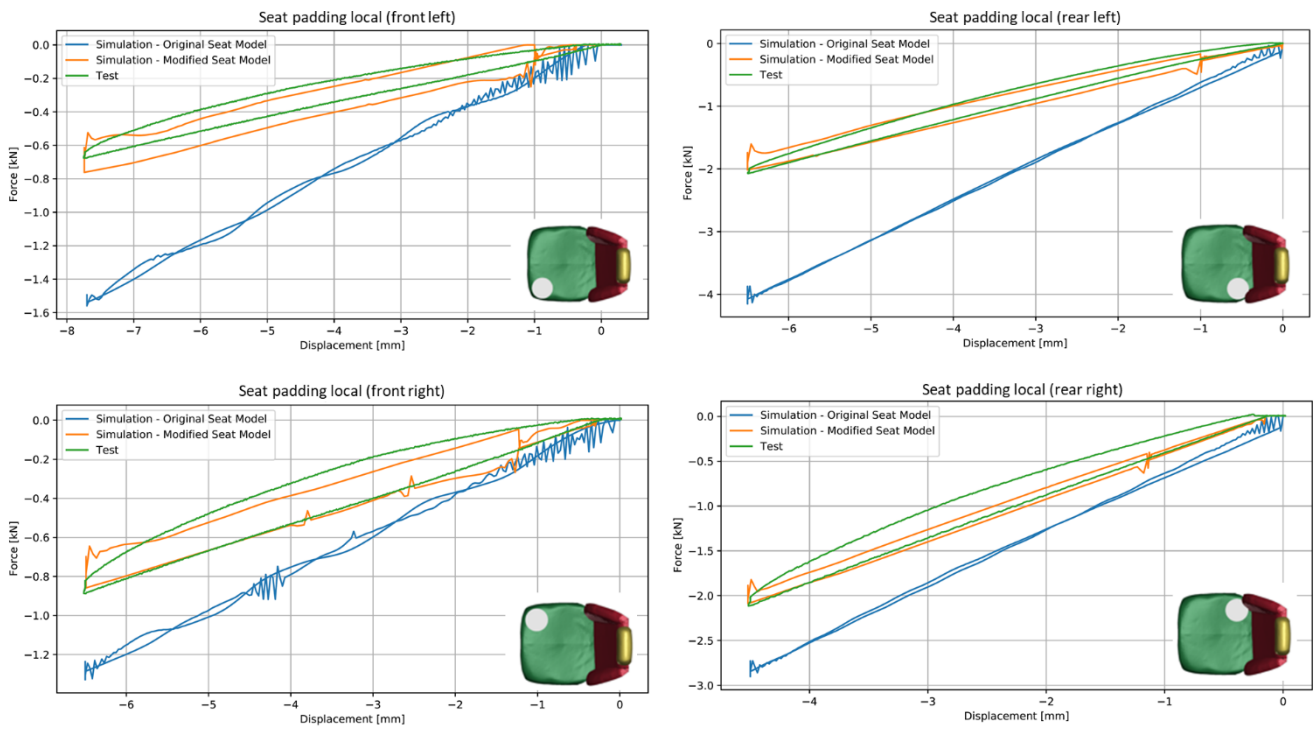

Fig. G-2. Force-displacement responses of the test, the original seat model and the modified seat model for configuration seat padding local (front left, front right, rear left, rear right).

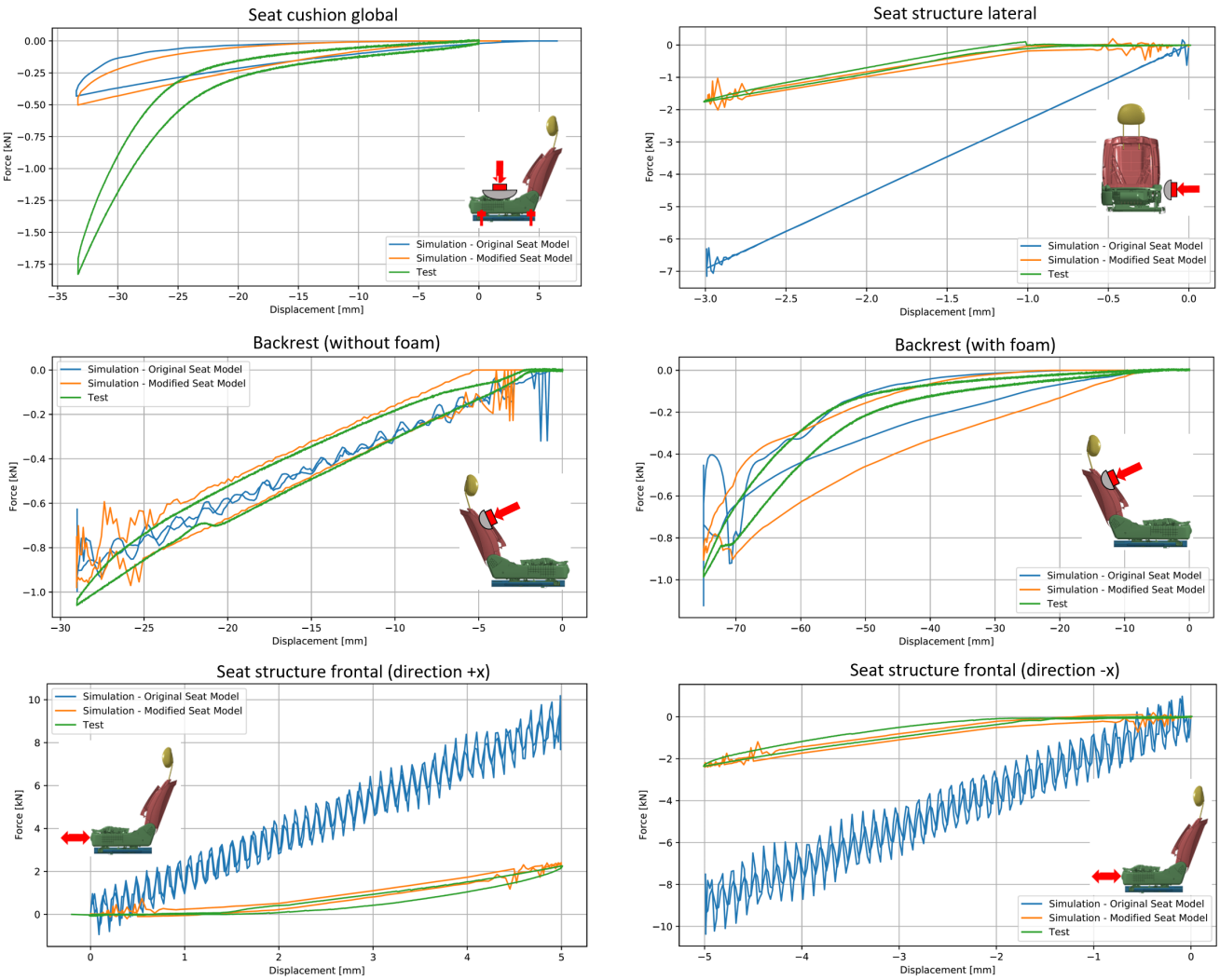

Fig. G-3. Force-displacement responses of the test, the original seat model and the modified seat model for configurations seat padding global, side structure lateral, backrest and seat structure frontal.